Role of Toothing on Out-of-Plane Behavior of Damaged Confined Masonry Walls

V. Singhal & D.C. Rai
Department of Civil Engineering, Indian Institute of Technology Kanpur, India

15 WCEE
LISBOA 2012

SUMMARY:
Load-carrying capacity of confined masonry walls in the out-of-plane direction after being damaged is crucial for overall stability and is affected by the type of interface present at the wall edge and column, such as toothing. Shake table tests were conducted to investigate the effectiveness of toothed connection on the out-of-plane behavior of damaged confined masonry walls. Three half-scaled clay brick masonry walls were subjected to a sequence of slow cyclic in-plane drifts and shake table-generated ground motions in the out-of-plane direction. Specimens included one regular RC infill frame and two confined masonry panels with different density of toothing. The specimen with infill panel demonstrated higher risk of out-of-plane collapse whereas the other two specimens with toothed connection maintained structural integrity and out-of-plane stability even when severely damaged. The toothing connections enhance the interaction between masonry walls and RC confining elements and were able to delay the failure by controlling out-of-plane deflections even after in-plane drift cycle of 1.75%.

Keywords: Confined Masonry, Seismic Performance, Shake-Table Test

1. INTRODUCTION

Confined masonry wall consists of masonry panel confined with horizontal and vertical reinforced concrete (RC) elements, namely tie-beams and tie-columns. The confined masonry is considerably different from infilled masonry RC frame with respect to *i*) construction methodology, as masonry wall is laid before column and *ii*) load transfer mechanism under gravity and lateral load. Such type of masonry is included in various building codes, such as the Mexico Building Code, the Eurocode, etc. (Brzev 2008). The structural behavior of confined masonry panels depends on their individual components: the frame is strengthened by the masonry to form a shear resisting element and, in turn, the masonry panel is strengthened by the beneficial containment of the frame. After the initial cracking of wall panel, the frame prevents the masonry from disintegrating because of its confining action. Thus, the coupled system has a high level of stiffness and strength from the masonry panel and ductility from the surrounding frame. Such construction has been evolved based on its satisfactory performance in past earthquakes (Brzev, 2008).

The in-plane performance of confined masonry has attracted considerable interest in seismic research. The summary of experimental studies conducted to understand the in-plane behavior of confined masonry walls in past three decades is presented by Meli et al. (2011). It was observed that confined masonry panels provide fair in-plane shear capacity and ductility and its behavior can be significantly affected by tie-column-to-wall interface, spacing and cross-section detailing of tie-column. Though commonly recognized as an effective practice, a little effort has yet been made to understand the out-of-plane behavior of confined masonry walls (Komaraneni et al., 2011).

Moreover, during an earthquake, the masonry panels are subjected to in-plane and out-of-plane loads simultaneously. The out-of-plane load-carrying capacity of these masonry panels may be substantially weakened after being damaged, endangering their overall safety and stability. The extent of damage and likelihood of wall collapse in the out-of-plane direction also depends on the type of floor diaphragm (rigid or flexible), and their connection with adjacent confining elements. Good bonding between the masonry wall and adjacent RC tie-columns is essential for satisfactory earthquake performance, and for delaying undesirable cracking and separation of wall with confining elements. Research study by Wijaya et al. (2011) observed that the wall-frame connection details play a crucial role in the in-plane load carrying capacity of confined masonry walls. The shake table test on confined masonry walls conducted by Tu et al. (2010) concluded that the strong boundary connection prevent masonry panel from falling out of the frame and thus can sustain considerable out-of-plane seismic loads.

The present study is an extension of the research in this area. It considers dynamic out-of-plane loading of cracked masonry at different in-plane damage levels. This paper describes the preliminary results of the experimental research undertaken to study the effect of toothing on behavior of confined masonry panels under simulated out-of-plane ground motions with prior in-plane damage.

2. EXPERIMENTAL PROGRAM

2.1. Specimen Details

The experimental work involved three half-scaled wall specimens as shown in Fig. 2.1. The prototype wall was taken to be half-brick thick wall with dimensions of 5 m long by 3 m high, which reduces to 2.5 m × 1.5 m for half-scaled test specimens. All the specimens are designed according to norms of the Mexican code (NTC-M, 2004). An intermediate tie-column was provided so that their spacing should be less than 1.5*h* or 2 m (for half-scaled specimen). For 60 mm thick half-scaled wall (slenderness ratio, h/t = 22.8), tie-column and tie-beam with 65 mm × 65 mm cross section was used for all specimens. First specimen S1 was regular masonry infilled RC frame in which the masonry wall was built after the RC frame. In other two specimens S2 and S3, the confining (frame) elements were constructed after the masonry wall and toothed edges were left on each side of the wall panel at the interface with the tie-column. To evaluate the effect of density of toothing, two different variations were examined; in specimen S2 the height of toothed edges was provided equal to thickness of two brick course (= 94 mm), whereas in specimen S3 it was equal to thickness of one brick course (= 47 mm). The toothing length equal to one-half of the brick unit length, *i.e.*, 60 mm was provided in both specimens S2 and S3 as shown in Fig. 2.1b and 2.1c.

The details of the geometry and reinforcement are summarized in Fig. 2.1. The masonry panel of all specimens were laid in stretcher bond using solid burnt clay bricks. Generally, prototype masonry has a mortar joint thickness in the range of 10 mm – 12 mm, so to satisfy the length ratio of the models, they should have had a mortar joint thickness of 5 mm – 6 mm. However, due to practical difficulties, an average thickness of 7 mm was obtained for all joints.

2.2. Material Properties

Micro-concrete of mix proportion 0.50:1:2.75 (water: cement: aggregate) was used in all RC members of specimens S1, S2 and S3. The average compressive and tensile strength of micro-concrete at 28 days was found to be 38.1 MPa and 3.5 MPa, respectively. Specially made half-scaled burnt clay bricks (120.4 mm × 61.8 mm × 38.5 mm) and a lime-cement mortar mix of 1:1:6 proportion (cement: lime: sand) was used for the masonry panels. The average compressive strength of the bricks and mortar mix was found to be 33.9 MPa and 6.89 MPa (28-days strength), respectively. For all specimens 6 mm and 3 mm diameter steel wires were used as longitudinal and transverse reinforcement in tie-beams and columns, respectively. Masonry prisms of five bricks tall were made when the brick wall was laid and were moist cured for 28 days before testing. The average compressive strength and modulus of elasticity of the masonry prisms was found to be 9.31 MPa (COV 11.3%) and 2843 MPa (COV 6.1%), respectively.

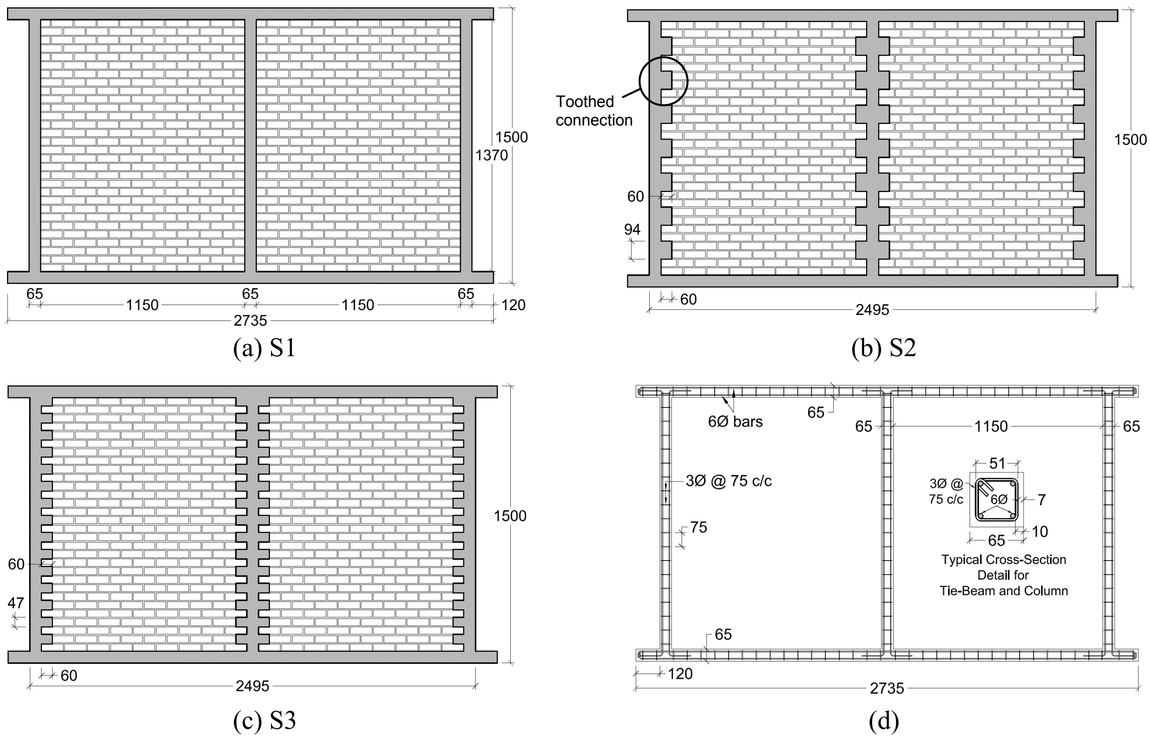

Figure 2.1 (a) – (c) Geometric details of test specimens and (d) Typical reinforcement details for tie-beam and tie-column

2.3. Artificial Mass Simulation

For a reliable correlation study with the prototype, one of the most important considerations is the appropriate modeling as per relevant similitude relations. Simulation of forces includes both gravitational and inertial types, which can be achieved by adding structurally ineffective lumped masses (Mills et al., 1979). For out-of-plane ground motions, the inertia forces are predominant forces on masonry wall panels and may cause instability in the walls, especially in slender walls with large height-to-thickness ratios. In this particular case, the artificial mass should also be distributed throughout, as the resulting inertia forces are uniformly distributed. Consequently, for half-scaled model bricks, the additional mass added for each brick in the wall is equal to the mass of that brick. Since the mass of a typical brick was approximately 0.435 kg, a lead block with a diameter of 60 mm, a height of 28 mm, and a weight of 0.865 kg, was attached to the wall in order to serve as artificial mass for two bricks. The lead blocks were mounted on steel bolts with a diameter of 4 mm that were fixed in a hole drilled into the facing side of bricks. These lead blocks were arranged in a regular grid pattern on both faces of the wall to eliminate any eccentric loading in the out-of-plane direction.

3. TEST SETUP

The unique testing method developed by Komaraneni et al. (2011) was used in this study, which involved successive applications of out-of-plane and in-plane loading, so that there was no need to move the specimen for the repeated cycles of loading in-plane and out-of-plane directions. The test setup for the out-of-plane and in-plane loading are shown in Figs. 3.1 and 3.2. However, some modifications were made from previous test set-up to improve the stiffness of lateral supports in the out-of-plane direction and fixity of test wall for overturning and sliding during in-plane loads. A 1.8 m × 1.2 m servohydraulic-driven uniaxial shake table was used for the out-of-plane loading (Sinha and Rai, 2009). For in-plane loads, four bars with a diameter of 20 mm were used to connect both ends of the top beam with a 250 kN servohydraulic actuator. The simulation of realistic boundary conditions is an important aspect of the subassemblage tests. In this study, the desired boundary conditions of diaphragm flexibility and deformations of the perpendicular walls were achieved by providing a sufficient number of lateral supports as shown in Figs. 3.1 and 3.2. The lateral supports provided on both sides of the wall were braced at the top to ensure sufficient torsional restraint to the RC beams and masonry walls during both in-plane and out-of-plane loading. The in-plane supports were attached to the strong-reaction floor to transfer overturning loads generated during the in-plane loading without overstressing the shake table bearings. In order to simulate gravity loads on the masonry panels, a vertical precompression force of 0.10 MPa was applied over the wall specimen with the help of a flexible wire rope arrangement.

For out-of-plane tests, 20 accelerometers were used: 18 were attached to the wall, one was fixed to the shake table and another was placed at the centre of top tie-beam. Four load cells were kept to measure variations in the vertical compressive load on the wall during testing. For both in-plane and out-of-plane tests, sufficient numbers of linear variable differential transducers (LVDT) and wire potentiometers were provided to monitor the wall displacement. A high-performance data acquisition system was used to collect data from sensors at a rate of 200 samples per second.

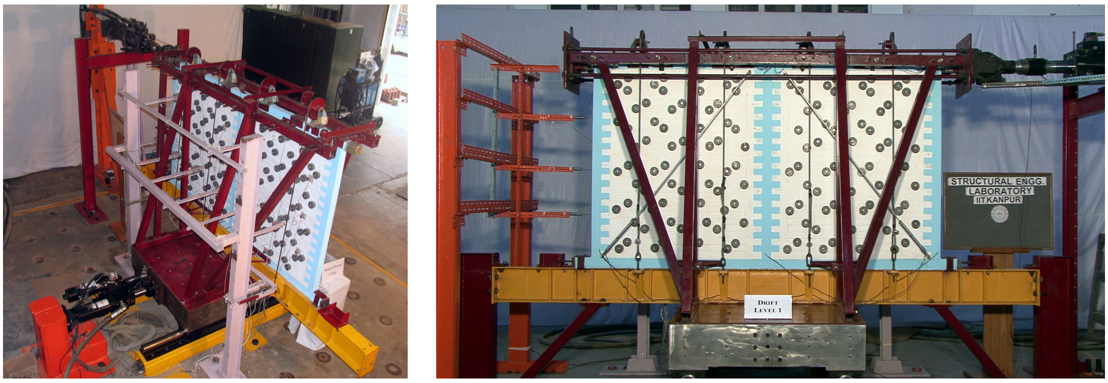

(a) (b)

Figure 3.1 Test setup for (a) out-of-plane loading and (b) in-plane loading

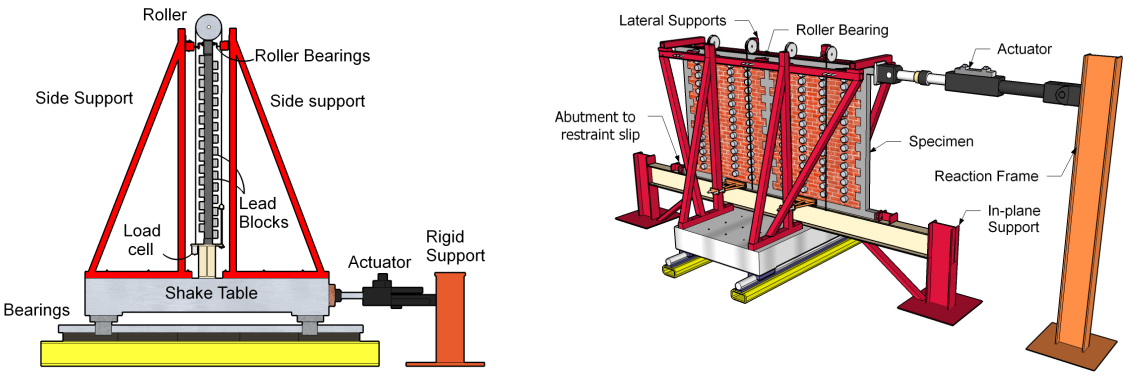

(a) (b)

Figure 3.2 Schematic showing various components of the test setup for (a) out-of-plane and (b) in-plane loading

3.1. Loading History

The specimens were subjected to simulated earthquake ground motions generated by a shake table in the out-of-plane direction. The N21E component of the 1952 Taft earthquake was chosen for the out-of-plane target ground motion, with a PGA of 0.156*g*. The first 30 s of ground motion was considered for the simulation (Fig. 3.3a), which included the strong motion portion and the time axis of the accelerogram was compressed by a factor of $1/\sqrt{2}$ to satisfy the dynamic similitude relations.

The 5% damped response spectrum of the Taft ground motion input was compared with the scaled design response spectrum specified in the IS 1893 (BIS, 2002) for a design earthquake in Zone V

(PGA = 0.36*g*), and a reasonable match was observed when the Taft motion was scaled to make its PGA equal to 0.40*g*, as shown in Fig. 3.3b. Also, the response spectra of the recorded Taft motion at the top of the shake table after appropriate tuning corresponded well with that of the original ground motion scaled to 0.4*g*, as shown in Fig. 3.3b and 3.3c. This ground motion is referred as Level V motion. Similarly, the Taft motion is scaled to a corresponding Zone II, III and IV of Indian seismic code and referred as Level II, III, and IV motions, respectively. A low-intensity white noise test (0.05*g*) was also conducted to investigate the change in the stiffness properties of the specimen after each cycle of the Taft earthquake motion. In-plane loading consists of displacement controlled slow cycle as per ACI 374.1-05 (ACI, 2006). This loading history consists of gradually increased storey drifts (displacements) of 0.20%, 0.25%, 0.35%, 0.50%, 0.75%, 1.00%, 1.40% and 1.75%. Each displacement cycle was repeated for three times at each drift ratio.

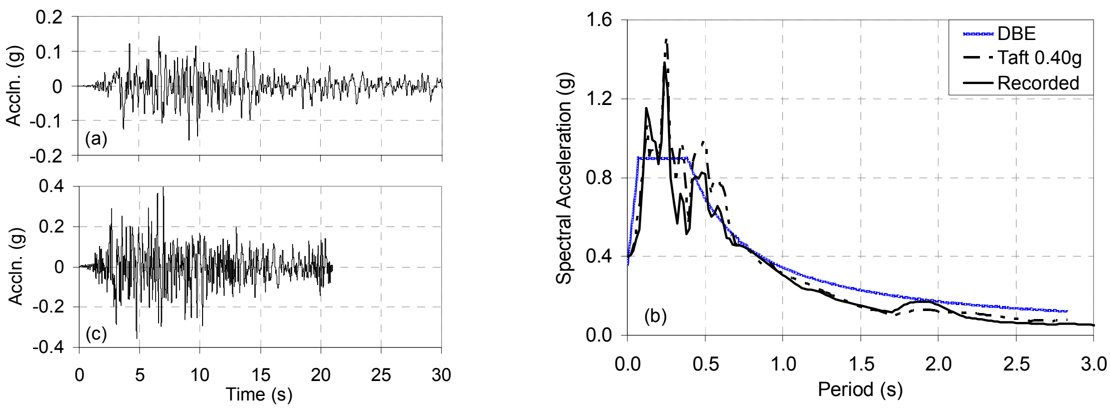

Figure 3.3 (a) TAFT N21E ground motion (b) Comparison of scaled response spectra of DBE (Design Basis Earthquake), original TAFT motion upscaled to 0.4g and recorded TAFT motion at table top surface. (c) Scaled TAFT motion recorded at shake table top surface

3.2. Test Procedure

After safely mounting the specimen on the shake table, forced vibration tests were performed to obtain the initial dynamic characteristics of the specimens. The load test started with the out-of-plane shake table motions consisting of a series of incremental Taft motions from Level I to Level V, with the white noise tests in between. After the completion of this out-of-plane loading schedule, the specimen was subjected to quasi-static in-plane cyclic loading. The in-plane cyclic loading was continued until cracks were visible, which was observed at the 0.50% drift cycle for all specimens. After this drift level, the second cycle of out-of-plane loading was applied which consisted of Level V Taft motion only, preceded and followed by white noise loading. The second cycle of in-plane loading was performed (drift ratio 0.75%) and an alternate process of out-of-plane and in-plane loading was continued until the specimen failed, as shown in Fig. 3.4. Visual observations were noted after each cycle of testing and the cracks in the specimen were marked.

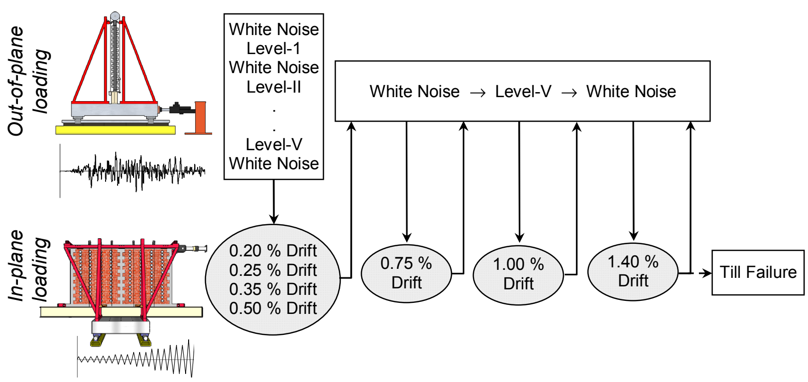

Figure 3.4 Summary of test procedure and loading sequence

4. RESULTS AND DISCUSSION

4.1. Physical Observation during the Testing

A majority of the cracks were formed due to the in-plane loading, while not many new cracks were observed during the out-of-plane loading. In subsequent loading cycles, the cracks formed at the initial stages of in-plane loading widened, and energy dissipation was mainly due to the sliding of masonry blocks along bed joints. In all specimens, the diagonal bed joint crack propagated from one load corner to another along with horizontal sliding, which eventually led to the formation of plastic hinges at the column ends and subsequent failure of exterior tie-column at higher drift level. The failure patterns of all three specimens are illustrated in Figs. 4.1 and 4.2. The specimen S1 with infill masonry showed separation of masonry wall with RC tie-beams and tie-columns even at in-plane drift level of 0.5%. However, specimens S2 and S3 with toothed connection did not experienced any such separation till the last drift cycle of 1.75% (Fig. 4.2b and 4.2c). These specimens showed uniformly distributed cracks formed in a stepped manner with sliding taking place at multiple bed joints. Due to the extensive cracking of the bottom of the masonry subpanels, inelastic activities were observed in both exterior tie-columns with rocking of masonry panels at higher drift levels.

Specimens S1, S2, and S3 reached their respective peak in-plane strengths of 86.1 kN, 92.2 kN and 107.8 kN. The first specimen showed significant out-of-plane deflection and arching after being subjected to a 1.75% in-plane drift and was on the verge of possible collapse due to overturning of wall panels (Fig. 4.1a). However, specimen S2 and S3 did not experienced large out-of-plane deflection even after 1.75% in-plane damage cycle and the test was stopped after this drift cycle due to fracture of longitudinal reinforcing bar in the exterior tie-columns. No appreciable difference in overall behavior was noted in specimens S2 and S3, suggesting that both types of toothing were nearly equally effective.

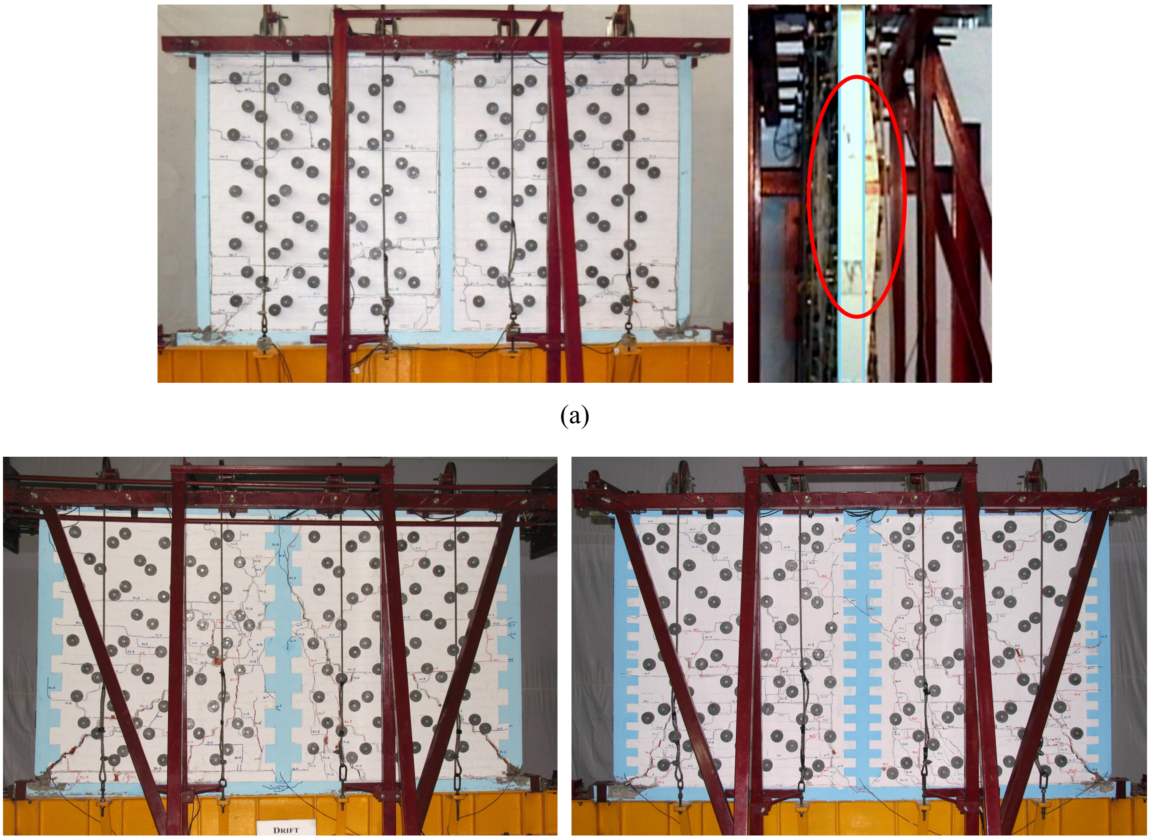

(a)

(b) (c)

Figure 4.1 Cracking pattern after 1.75% in-plane damage (drift) cycles for specimen (a) S1 with arching phenomenon under out-of-plane shake table motion, (b) S2 and (c) S3

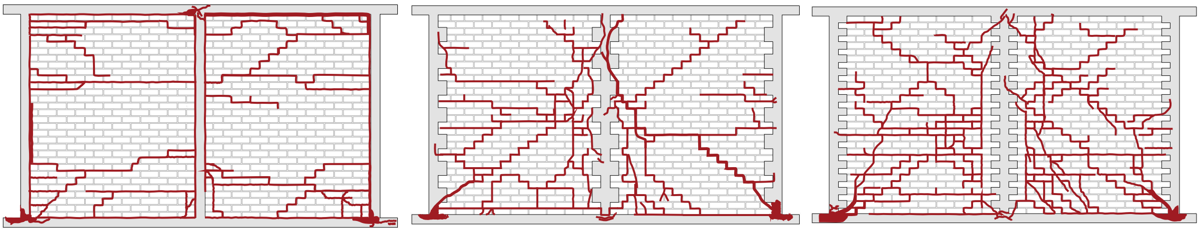

(a) S1 (b) S2 (c) S3

Figure 4.2 Comparison of cracking patterns for all specimens after 1.75% in-plane damage cycle

4.2. Effect of Toothed Connections

4.2.1. Out-of-Plane Behavior of Damaged Walls

The variation of equivalent uniform pressure (calculated from observed inertia forces) and average peak out-of-plane displacement at mid-height in each panel with in-plane drift (damage) is shown in Fig. 4.3a and 4.3b, respectively. The equivalent uniform pressure was calculated as follows: Peak acceleration at each location (18 accelerometers mounted on wall) was multiplied by the corresponding tributary mass to obtain peak inertial force, which was summed over all locations and then divided by the wall area. All specimens experienced relatively small variations in uniform pressure during the out-of-plane motion. As observed from Fig. 4.3a, the specimen S1 reached its peak uniform pressure in an undamaged state and once damage was introduced, the acceleration response decreased with continued in-plane damage except after 1.4% in-plane drift. The specimen S2 and S3 experienced increase in uniform pressure after few particular in-plane drift cycles, which may be due to higher local acceleration resulted from rocking of damaged masonry fragment. Conversely, the maximum out-of-plane displacement for specimen S2 and S3 remains fairly constant with in-plane damage (Fig. 4.3b). However, specimen S1 with infilled masonry showed continuous increase in out-of-plane deflection with in-plane damage and was likely to collapse after 1.75% drift cycle. This indicates that the observed out-of-plane instability was primarily due to excessive deflections, not governed by the accelerations (inertia forces).

The confined masonry wall specimens with toothing at the wall-to-tie column interface were quite effective in reducing out-of-plane deflections, and hence, in delaying the out-of-plane catastrophic failure by dislodgement, even beyond an in-plane drift of 1.75%. However, no significant difference in out-of-plane behavior for different arrangements of toothing in S2 and S3 was noted. Due to the presence of toothed edges, the composite action was developed between wall panel and tie-columns, as a result, the confined masonry wall behaved more like a shear wall with boundary elements and enhanced integrity of wall panel to columns helped reduce the likelihood of out-of-plane instability.

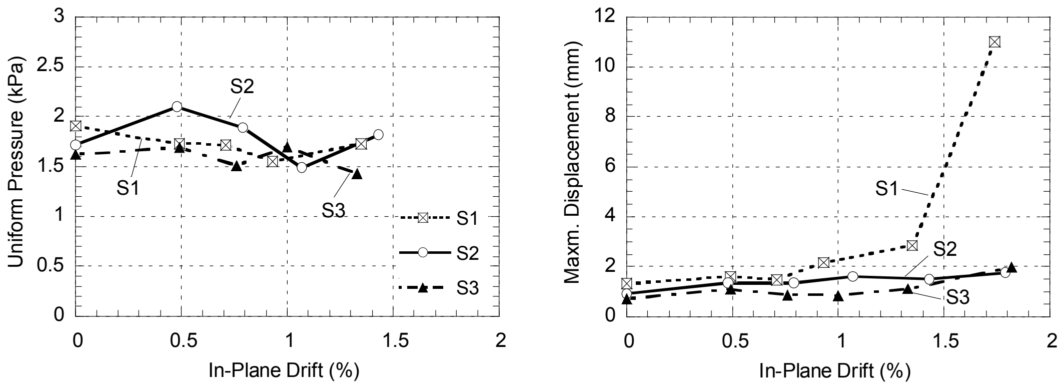

(a) (b)

Figure 4.3 (a) Variation of peak uniform acceleration and (b) out-of-plane displacement with in-plane drift (Damage)

Before and after each out-of-plane ground motion excitation, a white noise test run was performed to determine the natural frequencies of vibration. These tests often showed a decrease in the natural frequencies after each in-plane damage state, indicating the softening of the specimen due to accumulated damage during the test. The undamaged specimens had initial fundamental natural frequencies of 13.4 Hz, 15.8 Hz, and 14.8 Hz for specimens S1, S2, and S3, respectively. The slight increase in the natural frequencies of specimen S2 and S3 may be due to the increase in stiffness on account of toothing. As shown in Fig. 4.4, the total reduction in the fundamental frequencies before failure was 76.2%, 30.5%, and 17.9% for specimen S1, S2 and S3, respectively. It was observed that specimen S1, experienced sharp decrease in natural frequency with the in-plane damage. In contrast, specimen S2 and S3 showed a nearly constant rate of drop in natural frequency throughout the test, which can be attributed to the beneficial effect of the toothed connection.

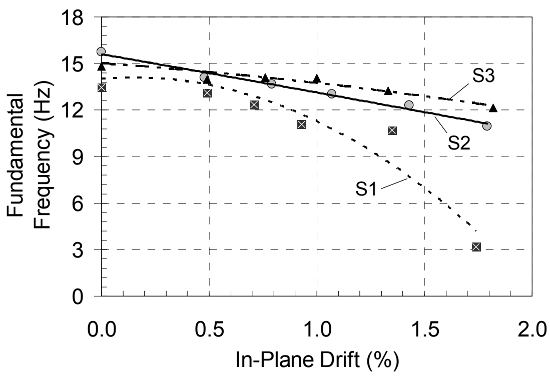

Figure 4.4 Variation in fundamental frequencies of the specimens

4.2.2. In-Plane Load-Displacement Response

The load-displacement hysteretic response and envelope backbone curves for all specimens are shown in Figs. 4.5 and 4.6a, respectively. The envelope backbone curve was obtained by joining the point of peak displacement during the first cycle of each increment of loading as indicated in ASCE/SEI 41-06 (2007). As observed from Fig. 4.5, the specimen S1 with masonry infilled RC frame showed relatively pinched hysteretic behaviour as compared to confined masonry specimen S2 and S3 with toothed connection. The toothing at the wall-to-tie-column interface moderately increases the in-plane resistance of masonry wall as compared to specimen S1 by 7% and 25% depending on the density (amount) of toothed edges. The sudden drop in in-plane load of specimen S2 in negative direction during drift cycle of 1% was due to accidental release of pretension in one of the flexible cable. To illustrate the stiffness degradation occurring between different loading sequences, cycle stiffness (K_i) as defined by Komaraneni et al. (2011) was estimated for each specimen as shown in Fig. 4.6b. It can be seen that cyclic stiffness steadily declined with each loading cycle and with the resulting accumulated damage. All specimen followed similar trends for stiffness degradation with in-plane drift cycle, however, specimen with toothed interface showed higher initial stiffness in the range of 12 – 28% as compared to infilled frame specimen.

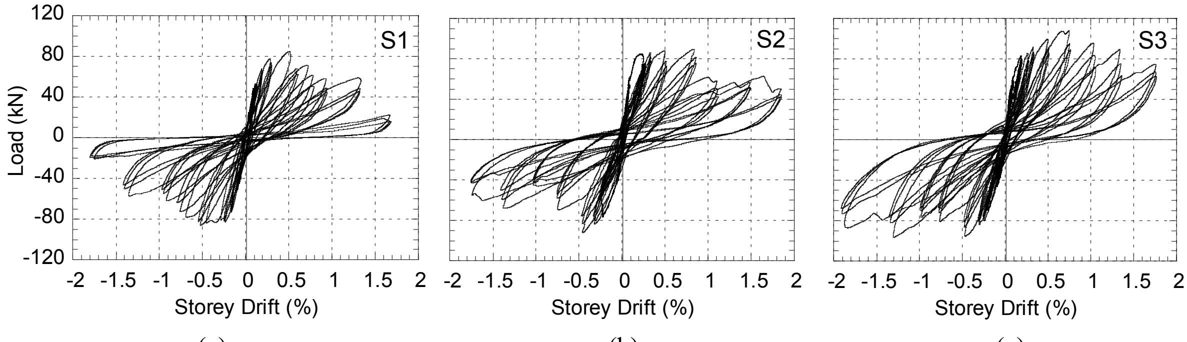

(a) (b) (c)

Figure 4.5 Hysteretic behavior of specimen (a) S1, (b) S2 and (c) S3

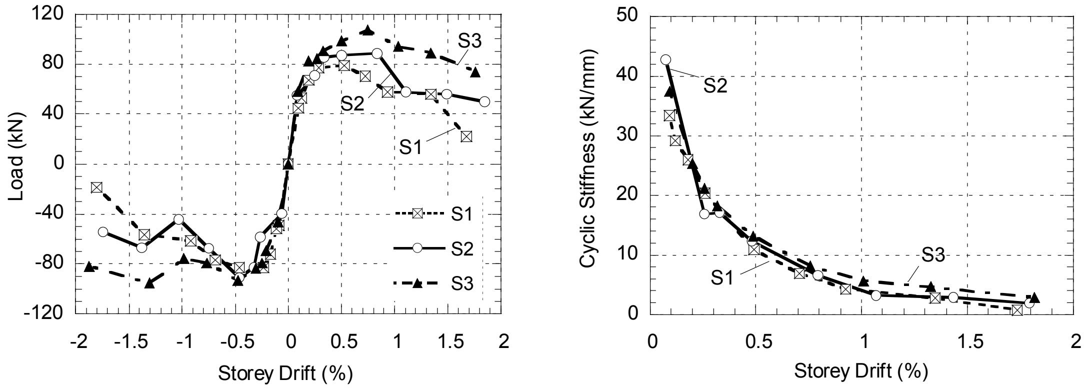

(a) (b)

Figure 4.6 Comparison of observed in-plane responses for all specimens (a) Envelope value of load versus story drift and (b) Cyclic stiffness against story drift

5. CONCLUSIONS

The study was concerned with the evaluation of out-of-plane response of confined masonry walls with toothed connection when damaged due to in-plane forces. Three half-scaled specimens of large slenderness ratio (*h/t* = 22.8) were observed to maintain structural integrity and out-of-plane stability under the design level out-of-plane inertial forces even in the damaged state caused by in-plane drifts in the excess of 1%. Toothing at the wall-to-tie-column interface clearly improved both in-plane and out-of-plane response. The increased density of toothing did not have significant effect on out-of-plane behaviour, however, it did cause moderate increase in in-plane strength. Under lateral load, walls with toothed connection acted as a shear wall and due to the composite action between wall and the tie-column, the out-of-plane failure was delayed and it could safely sustain large in-plane drifts upto 1.75%. However, RC frame with infill masonry showed the separation of wall panel at its interface with the framing element at in-plane drifts as low as 0.5%, which led to excessive out-of-plane deflection and increased risk of dislodgement from the frame. The exterior tie-column experienced extensive damage under in-plane drift cycles and, therefore, they need to be designed appropriately to carry large tensile forces generated due to overturning moments.

ACKNOWLEDGEMENTS

The financial support provided by the Ministry of Human Resource Development, Government of India is gratefully acknowledged. The authors sincerely appreciate the assistance received from the staff of the Structural Engineering Laboratory of the Indian Institute of Technology Kanpur.

REFERENCES

ACI. (2006). ACI 374.1-05: Acceptance Criteria for Moment Frames Based on Structural Testing and Commentary. American Concrete Institute, Farmington Hills, MI.

ASCE. (2007). ASCE/SEI 41-06: Seismic rehabilitation of existing buildings. American Society of Civil Engineers, Reston, VA.

Brzev, S. (2008). Earthquake-Resistant Confined Masonry Construction. National Information Center of Earthquake Engineering, Indian Institute of Technology Kanpur, India.

BIS. (2002). IS 1893: Indian Standard Criteria for Earthquake Resistant Design of Structure, Part 1: General provisions and buildings. Bureau of Indian Standards, New Delhi, India.

Komaraneni, S., Rai, D. C. and Singhal, V. (2011). Seismic Behavior of Framed Masonry Panels with Prior Damage when Subjected to Out-of-Plane Loading. *Earthquake Spectra,* **27:4**, 1077-1103.

Meli, R., Brzev, S., Astroza, M., Boen, T., Crisafulli, F., Dai, J., Farsi, M., Hart, T., Mebarki, A., Moghadam, A. S., Quiun, D., Tomazevic, M. and Yamin, L. (2011). Seismic Design Guide for Low-Rise Confined Masonry Buildings. World Housing Encyclopedia, EERI and IAEE, [Online], Available: www. confined masonry.org/risk-management-solutions-supports-network/design-guideline-working-group [1 Nov. 2011]

Mills, R. S., Krawinkler, H., and Gere, J. M. (1979). Model Tests on Earthquake Simulators: Development and implementation of experimental procedures. *Report No. 39,* The John A. Blume Earthquake Engineering Center, Stanford University, CA.

NTC-M. (2004). Commentary Technical Norms for Design and Construction of Masonry Structures. Mexico D.F.

Sinha, P., and Rai, D. C. (2009). Development and Performance of Single-axis Shake Table for Earthquake Simulation, *Current Science*, **96:12**, 1611–1620.

Tu, Y. H., Chuang, T. H., Liu, P. M., and Yang, Y. S. (2010). Out-of-Plane Shaking Table Tests on Unreinforced Masonry Panels in RC Frames. *Engineering Structures*, **32**, 3295-3935.

Wijaya, W., Kusumastuti, D., Suarjana, M., Rildova and Pribadi, K. (2011). Experimental Study on Wall-Frame Connection of Confined Masonry Wall. *Procedia Engineering*, **14**, 2094-2102.